Proceedings of the ASME 2016 International Mechanical Engineering Congress and Exposition
IMECE2016
November 11-17, 2016, Phoenix, Arizona, USA

IMECE2016-66855

ELECTRO-MECHANICAL IMPEDANCE MEASUREMENTS IN AN IMITATED LOW EARTH ORBIT RADIATION ENVIRONMENT

Mary L. Anderson
New Mexico Institute of Mining & Technology
Socorro, New Mexico, United States

Joshua D. Daniel
White Sands Missile Range
Las Cruces, New Mexico, United States

Andrei N. Zagrai
New Mexico Institute of Mining & Technology
Socorro, New Mexico, United States

David J. Westpfahl
New Mexico Institute of Mining & Technology
Socorro, New Mexico, United States

ABSTRACT

Piezoelectric sensors are used in many structural health monitoring (SHM) methods to interrogate the condition of the structure to which the sensors are affixed or imbedded. Among SHM methods utilizing thin wafer piezoelectric sensors (PWAS), electro-mechanical impedance monitoring is seen as a promising approach to assess structural condition in the vicinity of a sensor. Using the converse and direct piezoelectric effects, this health monitoring method utilizes mechanical actuation and electric voltage to determine the impedance signature of the structure. If there is damage to the structure, there will be a change in the impedance signature. It is important to discern between actual damage and environmental effects on the piezoelectric ceramic sensors and the structure. If structural health monitoring is to be implemented in space structures on orbit, it is imperative to determine the effects of the extreme space environment on piezoelectric sensors and the structures to which they are affixed. The space environment comprises extreme temperatures, vacuum, atomic oxygen, microgravity, micro-meteoroids and debris, and significant amounts of radiation. Radiation in space comes from three sources: solar events, background cosmic radiation, and trapped particles in the Van Allen Belts. Radiation exposure to structures on orbit will vary significantly depending on the duration of the flight and the altitude and inclination of the orbit. In this contribution, the effect of gamma radiation on piezoelectric ceramic sensors and space grade aluminum is investigated for equivalent gamma radiation exposure to 3-months, six-months, and 1-year on Low Earth Orbit (LEO).

An experiment was conducted at White Sands Missile Range, Gamma Radiation Facility using Cobalt-60 as the source of radiation. A free PWAS and a PWAS bonded to a small aluminum beam were exposed to increasing levels of gamma radiation. Impedance data were collected for both sensors after each radiation exposure. The total radiation absorbed dose was 200 kRad (Si) by the end of the experiment. The results show that piezoelectric ceramic material is affected by gamma radiation. Over the course of increasing exposure levels to Cobalt-60, the impedance frequency of the free sensor increased with each absorbed dose. The impedance measurements of the sensor bonded to the aluminum beam reflects structural and sensor's impedance. The data for this sensor show an increase in impedance amplitude with each level of absorbed dose. The mechanism at work in these impedance changes is suggested and future experimental work is identified. A survey of previous results of radiation exposure of piezoelectric ceramic sensors and aluminum alloys is presented and are compared to previous studies.

INTRODUCTION

The need to identify and repair damage to space structures has become increasingly important in order to reduce accidents and costs while maintaining viable, effective structures. Research into non-destructive evaluation (NDE) and structural health monitoring (SHM) methods has produced promising results using many techniques, among which are utilization of guided waves and electro-mechanical impedance to detect damage such as cracks or corrosion [1] [2] and inadequate assembly [3] or fatigue damage.

Damage detection in space structures is predominantly performed on Earth, before a structure enters orbit, because parts are manufactured, stored, and then shipped to the launch site for assembly. Damage may occur during any of these phases, so inspection is required before launch. However, currently, the most predominant method of "health monitoring" consists of visual inspection followed by non-invasive

examinations such as x-ray if damage is detected by the former method, a costly and time-consuming endeavor. It is important to verify that manufactured parts for space structures are flight-ready. But what about after launch? Can a health monitoring system be employed on a structure on orbit?

If structural health monitoring is to be used effectively in space structures on orbit, then such a system must withstand the effects of the extreme space environment. Structures on orbit will experience microgravity, atomic oxygen, extreme temperatures, vacuum, and radiation [4].

Radiation in Space

Radiation in the space environment comes from three major sources: solar particle radiation (from within the solar system), galactic cosmic radiation (from outside of the galaxy), and trapped particle radiation (from within the Van Allen Belts.) Much data have been compiled on the effect of high-particle radiation as it pertains to crewed missions and shielding. The greatest particle density emanates from the sun in the form of solar wind. Solar events contribute spikes in the particle flux. Protons comprise the bulk of the particle radiation from solar wind and solar events. The next most abundant particles are alpha particles, although heavy nuclei have been observed in the radiation from major solar events. Galactic cosmic radiation comes from beyond our solar system and is mostly fully-ionized nuclei which comprise up to a third of the interstellar energy density. These nuclei come from nearly all of the elements including the actinide group [4]. Radiation energy ranges from keV for trapped electrons in the Van Allen Belts to GeV for galactic cosmic radiation and solar heavy ions [5]. The particles trapped within the Van Allen Belts are protons and electrons. Even within the Van Allen Belts, radiation exposure can fluctuate by orders of magnitude in a magnetic storm [6]. A structure on low earth orbit (LEO) will encounter all of these forms of radiation to varying degrees, depending on the period in the solar cycle, and on the altitude and inclination of the orbit.

Simulating the Space Environment

Radiation in space is a complex mix of particles as well as secondary effects, making simulation of space radiation a difficult endeavor [7]. Naturally occurring radiation in the Solar system ranges in energy from 10 keV (for Van Allen Belts radiation) to over 30 MeV (for a solar event). Depending upon the purpose of the radiation simulation, approximations of space radiation can be adequately modeled. Cobalt-60 is used to simulate ionization effects that occur in space due to radiation and can produce the levels of radiation energy that occur within the Van Allen Belts [7]. Cobalt-60 is an unstable isotope that emits two photons of energy as it returns to stability. The first emission is approximately 1.173 MeV, and the second emission is approximately 1.332 MeV. High doses of gamma rays emanate from Cobalt-60 and can achieve ionization in a few hours that would take years in space. The rate in space for a high-radiation orbit is approximately 0.3 rad/hr [8].

SHM/NDE in Nuclear Reactors and Nuclear Waste Management

At the turn of the 21st century, researchers were considering structural health monitoring as a means to monitor nuclear reactors and nuclear waste sites [9]. In little more than a decade, SHM was being implemented in some areas of nuclear reactors [10] and nuclear waste management [11]. Researchers are testing and creating high-temperature piezoelectric ceramics that can survive in harsh environments [12].

In nuclear waste sites, the monitoring system is expected to endure gamma radiation and must be durable enough to last a century [11]. Many sites use pressure differential monitoring and continuous air monitoring (CAM) which do not constitute structural health monitoring or non-destructive evaluation of critical infrastructure. These methods serve as notification that a leak has occurred [13]. The Waste Isolation Pilot Plant (WIPP) near Carlsbad, New Mexico uses piezometers and extensometers to monitor movement or drift in the tunnels where waste is stored, but there is no monitoring of the actual nuclear waste containment [13]. There are non-destructive evaluation (NDE) systems available commercially for nuclear power plants, but they are labor-intensive and limited to accessible areas of the plants, although typically more accurate than continuous monitoring systems [10].

Radiation Effects on Piezoelectric Ceramic Sensors

The effect of radiation on piezoelectric ceramic sensors is of interest in the development of continuous structural health monitoring methods such as the electro mechanical impedance method. In the aforementioned method, piezoelectric sensors are bonded or imbedded in a structure, and a mechanical wave is sent through the material that allows for the inferring of structural dynamic characteristics that, due to the direct piezoelectric effect, are reflected in electro-mechanical impedance of a piezoelectric sensor. If there is damage to the structure, there will be a change in structural dynamics signature, and hence, in impedance measured by piezoelectric sensor [14]. If piezoelectric sensors are considered for operation in radiation environments, then understanding the effects of radiation on piezoelectric ceramics is imperative.

In 1965, Glower et al. investigated radiation on lead-zirconate-titanate (PZT) ceramics in high neutron flux and gamma radiation. The researchers subjected the PZT ceramics to 3×10^{13} neutrons/cm^2 sec and 10^9 rad (H_2O)/hr. Remanent polarization began to decrease in the piezoelectric material. Polarization hysteresis loop changed from symmetric to asymmetric, then to anti-ferroelectric-type hysteresis [15]. Fifteen years later, Broomfield demonstrated that irradiation reduces capacitance and electromechanical coupling in PZT ceramics. Increase in resonant frequency was also detected [16]. Meleshko et al. tested different thicknesses of piezoelectric transducers in a reactor where the specimens were exposed to fast neutrons (E>1.15 MeV) and gamma radiation. In these tests, capacitance decreased for all thicknesses, but less

so in thicker specimens (4 mm.) Resistance decreased for all transducers regardless of thickness [17].

Recently, Lin et al conducted an experiment on the effects of radiation on one of the foundational elements of structural health monitoring systems—the piezoelectric wafer active sensor (PWAS). In this experiment, PWAS were subjected to gamma radiation. After eight hours of exposure, the piezoelectric sensors showed decreased operating temperature, decreased capacitance, and increased frequency breadth [18].

Radiation Effects on Aluminum Alloys

Aluminum is used in nuclear reactors due to its resistance to radiation effects. E. F. Sturcken investigated radiation effects on aluminum and magnesium alloys. The irradiation on the 6063 aluminum alloy consisted of 1.9 x 10^{22} neutrons/cm^2 > 0.2 MeV and 1.3 x 10^{22} neutrons/cm^2 >0.8 MeV for 30,235 MW (302.35 full-power days.) The 6063 aluminum experienced some density loss (0.2%), which was attributed to silicon precipitation due to nuclear transmutation. The radiation increased the yield strength and the ultimate strength of the aluminum but decreased ductility [19]. Kamigaki et al. explained that the evolution of structural damage in aluminum alloys [20] is caused by:

"• under-sized solute atoms in the alloys (Si and Li) accelerating the nucleation of interstitial loops by combining with interstitial atoms; and

• oversized solute atoms (Mg) accelerating vacancy clustering by combining with vacancies."

Hamaguchi and Dai demonstrated that an aluminum-magnesium alloy irradiated by protons showed significant microstructural changes—mainly, dislocation loops and the formation of helium bubbles throughout the material [21]. Almazouzi et al. state that irradiation with high-energy heavy ions produce Frenkel pairs (which are interstitials located adjacent to vacancies in lattices) and can dramatically affect the mechanical properties of metals [22]. Sindelar et al. explored material degradation and corrosion due to radiation. The researchers determined that aluminum alloys experience accelerated fatigue damage as a result of exposure to radiation [23].

Electro-Mechanical Impedance Spectroscopy in an Irradiated Environment

It is clear from the literature that radiation affects all aspects of the materials used in the SHM electro-mechanical impedance method. Different types of radiation produce interstitials and vacancies in piezoelectric ceramics and in aluminum alloys—both materials are used in electro-mechanical impedance spectroscopy (EMIS). One could use other alloys, but the effects of radiation are seen in many metals, even those specifically made for use in nuclear reactors. Although the materials have been investigated in radiation environment, and EMIS measurements taken, explanation of the mechanisms that cause the changes in impedance frequency PWAS are not reported [24]. It would be beneficial to perform EMIS in an irradiated environment and determine the effects on the impedance signature. The insights gained from such an experiment may make it possible to compensate for the effects of radiation with adequate modeling, making EMIS a useful tool even in irradiated environments such as space.

EXPERIMENT

The experiment was designed to identify the effects of gamma radiation on the SHM electro-mechanical impedance method at increasing levels of absorbed dose of gamma radiation. The test was performed at White Sands Missile Range (WSMR) Gamma Radiation Facility (GRF), and was designed to emulate radiation exposure of three months, six months and one year on low earth orbit (LEO) over the course of the experiment [25]. The radiation exposure is expressed in rad (Si)—radiation absorbed dose in silicon.

Samples and Sensors

Two beams machined from 6061-T6 aluminum were fitted with two piezoelectric wafer active sensors (PWAS) on each beam. PWAS were affixed with Hysol © aerospace-grade adhesive. One beam had fixed-fixed boundary conditions. One beam had fixed-free boundary conditions. One sensor was not affixed to a beam (free sensor). The two aluminum samples were affixed to a stainless steel plate with 25 in-lbs torque. The sensors are APC 851 lead-zirconate-titanate (PZT) piezoelectric wafer active sensors with the following dimensions: 6.9558 mm - diameter and 0.2527 mm - thickness. Two sensors are affixed to each sample beam with Hysol © aerospace-grade adhesive. The samples and the sensors are shown in Figure 1.

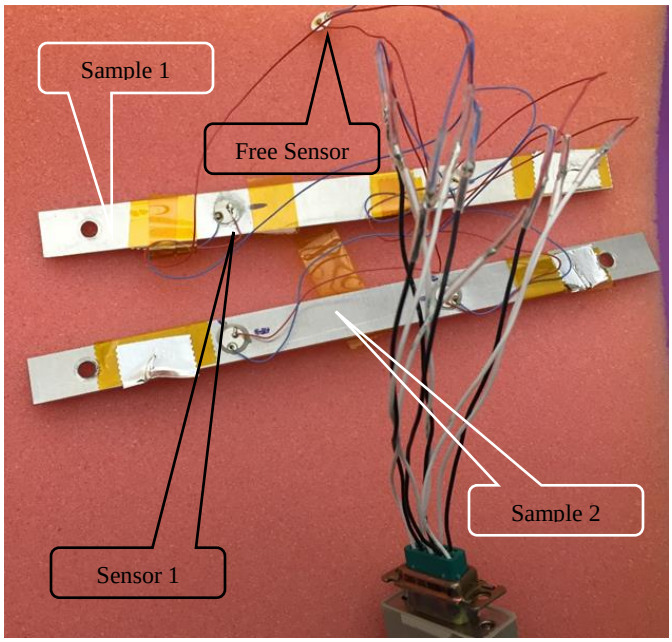

FIGURE 1. ALUMINUM BEAMS WITH PIEZOELECTRIC SENSORS AND THE FREE SENSOR.

Equipment

Cobalt 60 (Co-60) gamma irradiation facility, WSMR
And Fluke ion chamber 33cc (Figure 2)
with 3.2% calibration uncertainty.
Fluke ® Biomedical Advanced Therapy Dosimeter 35040
(Calibration due date: July 2016)
Thermoluminescent Dosimeters (TLDs) (Figure 3)
Kestrel ® 4000 Weather Tracker (Can be seen in Figure 4)
Cypher Instruments C-60 impedance analyzer with dedicated software.

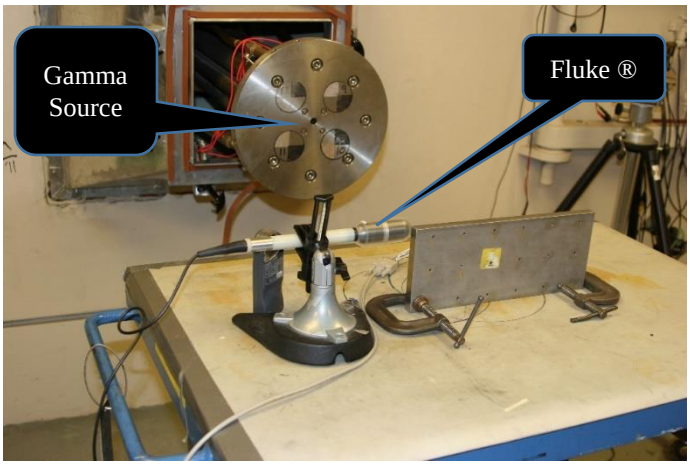

FIGURE 2. WHITE SANDS CO-60 RADIATION EQUIPMENT.

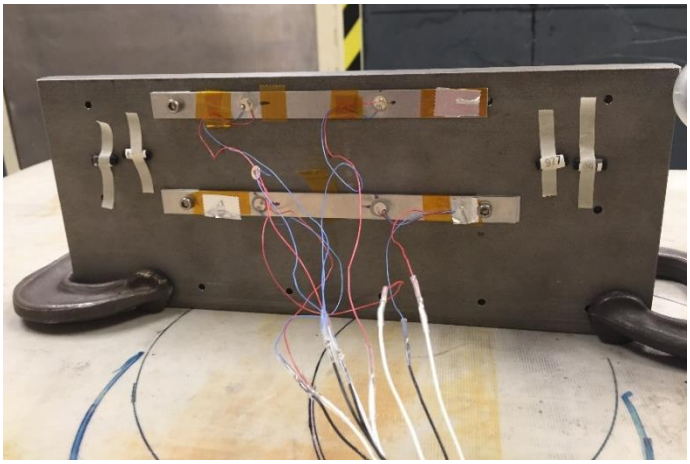

FIGURE 3. SAMPLES AFFIXED TO STEEL PLATE IN THE ION CHAMBER. TLDS ARE TAPED TO THE STEEL PLATE.

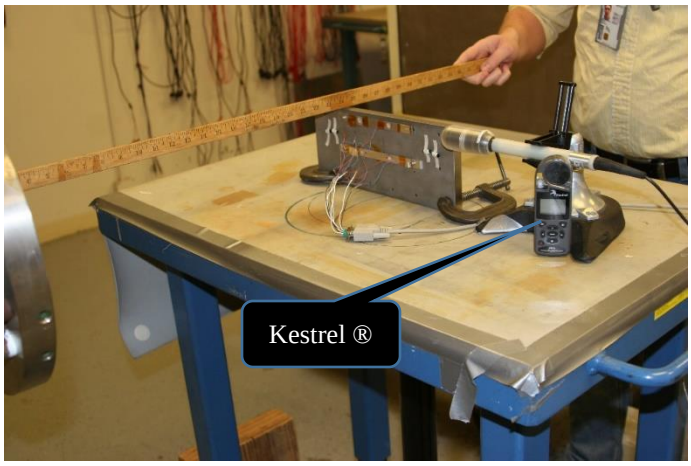

FIGURE 4. COMPLETE EXPERIMENTAL SETUP IN THE GAMMA RADIATION CHAMBER.

Thermoluminescent Dosimeters and Conversions

Materials absorb radiation differently. Absorbed dose is often reported as radiation absorbed dose in silicon (Rad (Si)). By utilizing Thermoluminescent Dosimeters (TLDs) we can estimate the absorbed dose. Manganese Calcium Fluoride (Mn:CaF2) is an ideal TLD material for this, because its response to gamma radiation very closely mirrors that of elemental silicon. The TLD measurement methods at WSMR are traceable from the National Institute of Standards and Technology (NIST), but there is an inherent uncertainty of about eight percent. The conversion factor used from Roentgen to Rad (Si) is 0.866. Methodology used for TLD testing, processing, and analysis follows all of the guidelines of the American Society of Testing and Materials (ASTM) E666 and E668.

Experiment Set Up

The samples were set inside of a Co-60 gamma irradiation facility on a standard metal testing table inside of a concrete irradiation cell. Fifty-five feet of serial cable with 9-pin connectors was run from the control room to the samples.

Mn:CaF2 TLDs were taped to the steel plate near the samples. Two TLDs were used for the first irradiation at 10 kRad (Si) and four TLDs were used for each irradiation thereafter. The TLDs were collected after each irradiation interval and replaced in the same locations with new TLDs.

Pre-test were conducted to ensure that a signal was obtained from each sensor. Two sensors were selected for the experiment: sensor one (S1) on the fixed-free beam and the free sensor, which was designated as sensor five (S5). The frequency range selected was 20 to 25 kHz for S1 and 200 to 250 kHz for S5. The assigned frequencies were transmitted to each of the two sensors for the duration of the tests.

The Fluke ion chamber was placed to the side of the samples at a distance of 24 inches from the irradiation source (as shown in Figure 4) to monitor the radiation and communicate to the Fluke dosimeter which was being continually monitored in the control room.

Irradiation Equilibrium

A distance of 24 inches from the irradiation source was selected to ensure adequate, uniform coverage of the samples. At this distance, there is minimal exposure gradient on the samples. No shielding was used to negate the down-scattered gammas, therefore, there are lower energy gammas also absorbing into the samples, and true equilibrium is not achieved. The down-scattered gamma particles have a negligible effect. The gamma peaks of interest from the Co-60, 1166 keV and 1333 keV are achieved and compose the majority of the gamma particles incident on the samples.

Cobalt Source Strength

The Co-60 sources were refueled in July of 2012. Each source was approximately 15 kilo-Curies (kCi) when refueled. Using the following equation we can calculate the approximate activity of the sources at the time of exposure: January 19, 2016.

$$A = A_0 e^{-\lambda t} \quad (1)$$

Where λ relates to the half-life, τ:

$$\lambda = \frac{\ln(2)}{\tau_{\frac{1}{2}}} \quad (2)$$

The half-life of Co-60 is 5.2714 years (1925.38 days). On the date of irradiation the sources were 1298 days from the initial fueling date. Using these values we calculate that each source is approximately 9.4 kCi. All four sources were used during irradiation, making the total activity of the source 37.6 kCi.

Target Exposure Levels

In order to achieve the target absorbed doses, the samples were irradiated for different time intervals ranging from 9 minutes to 25 minutes at an exposure rate of 1283 Roentgens/minute (1.11 kRad(Si)/min). The target total absorbed doses were identified as:

10 kRad (Si)	
25 kRad (Si)	
50 kRad (Si)	
75 kRad (Si)	Approximation of 3 months LEO
100 kRad (Si)	
125 kRad (Si)	Approximation of 6 months LEO
150 kRad (Si)	
200 kRad (Si)	Approximation of 12 months LEO

After each exposure interval, impedance measurements were taken from S1 and S5. The TLDs were retrieved and replaced. The next exposure interval was calculated.

The temperature and atmospheric pressure of the chamber was monitored throughout the experiment. The temperature at the beginning of the experiment was 16 °C. The barometric pressure was 26.01 in-Hg. These values are used as a correction factor for the ion chamber dosimeter.

Fig. 6-7 show raw impedance data, which was smoothed by spline interpolation. Procedure included locally weighted scatter smoothing (LOWESS) in Matlab ©. Spans were selected from 10 to 50 in increments of 10, then examined visually for best fit, which was determined by nearness to maximums and minimums in the raw data. A span of 30 was determined to be the best fit and is shown for sensor 5 in Figure 5. Resultant smoothed data is presented in Figure 10 for sensor 1 and in Figure 13 for sensor 5.

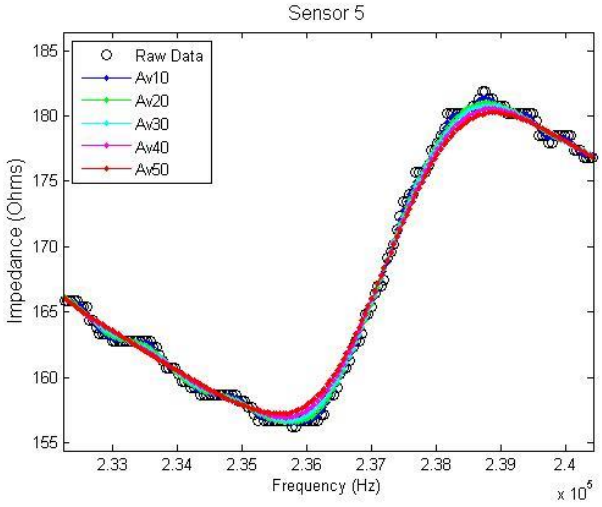

FIGURE 5. SENSOR 5 LOWESS SMOOTHING.

RESULTS

TABLE I. GAMMA RADIATION ABSORBED DOSE OVER THE ENTIRE SAMPLE PLATE.

Target Dose [Rad(Si)]	Target Exposure [R]	Actual Exposure [R]	Estimated Dose [Rad(Si)]	Actual Dose [Rad(Si)]	% Difference	Estimated Total Absorbed Dose [Rad(Si)]	Actual Total Absorbed Dose [Rad(Si)]	% Difference
10,000	11,547	11,494	9,954	-	0.00%	9,954	9,954*	0.00%
25,000	28,868	16,119	13,959	14,175	1.52%	23,913	24,129	0.90%
50,000	57,737	31,110	26,941	26,270	-2.56%	50,854	50,399	-0.90%
75,000	86,605	24,560	21,269	21,335	0.31%	72,123	71,734	-0.54%
100,000	115,473	33,100	28,665	28,040	-2.23%	100,788	99,774	-1.02%
125,000	144,342	28,710	24,863	25,370	2.00%	125,651	125,144	-0.40%
150,000	173,210	27,320	23,659	22,645	-4.48%	149,310	147,789	-1.03%
200,000	230,947	62,510	54,134	49,170	-10.09%	203,443	196,959	-3.29%

* TLD data at 10 kRad (Si) was not collected. Therefore, the estimated dose was used as the actual dose in calculating the total dose on the setup. It is reasonable to assume that the difference from the TLD reading and the ion chamber at this point would not exceed 3% based on other low exposure measurements.

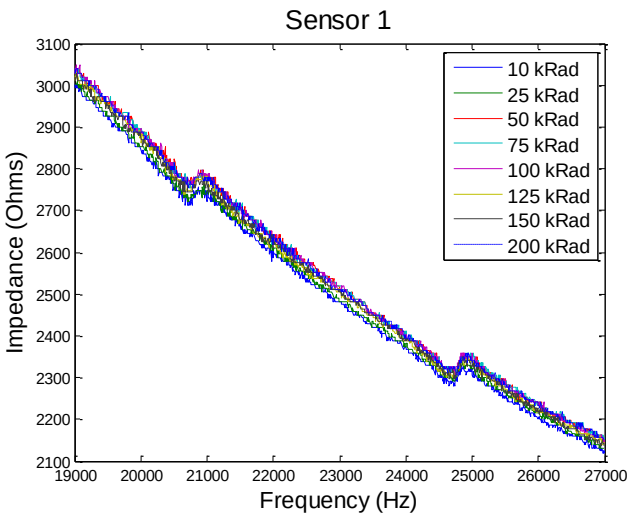

FIGURE 6. SENSOR 1 RAW IMPEDANCE DATA

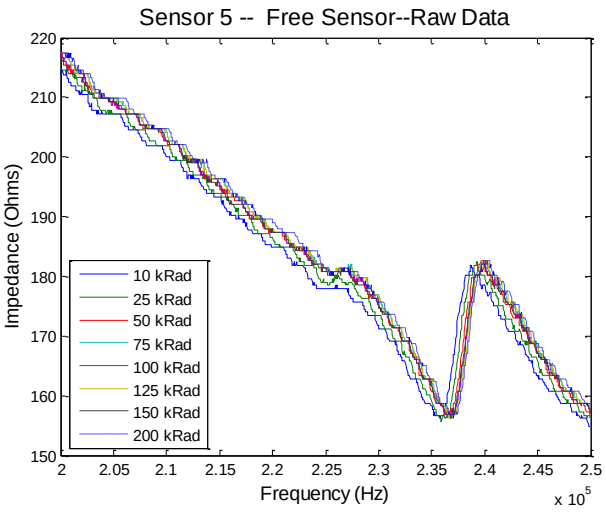

FIGURE 7. SENSOR 5 RAW IMPEDANCE DATA

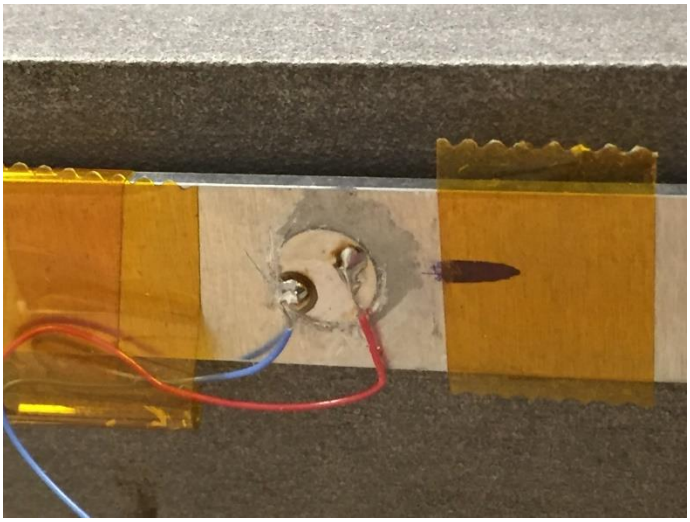

FIGURE 8. SENSOR 1 POST IRRADIATION

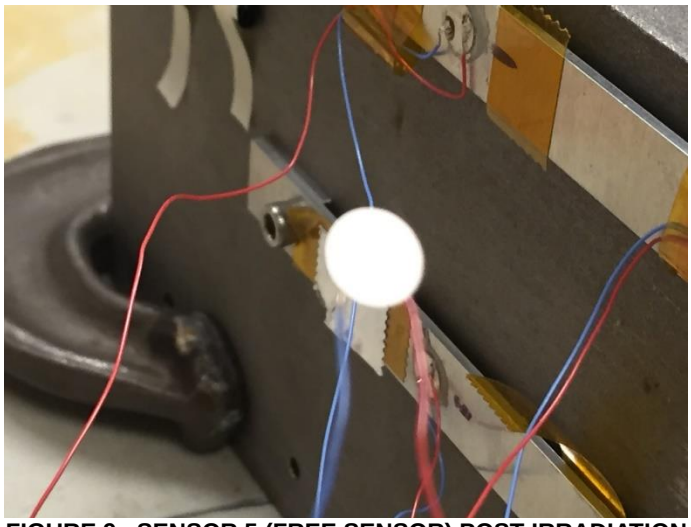

FIGURE 9. SENSOR 5 (FREE SENSOR) POST IRRADIATION

CONCLUSION

Sensor 1

From Figure 8 it can be seen that there is no visible damage to S1 or the surrounding aluminum. The flux from the solder of the sensor wires has darkened, but the solder is not damaged and the bond remains intact. Sensor 1 is considered to be perfectly bonded to the aluminum beam, and largely reflecting the impedance signature of the aluminum beam. As the samples are exposed to increasing gamma radiation, the amplitude of the impedance is affected, as shown in Figure 10. An increase in the amplitude of the signature indicates a decrease of sensor capacitance, which was observed before. In addition, damping may contribute to this process. It is possible that the adhesive bond is softening due to gamma radiation.

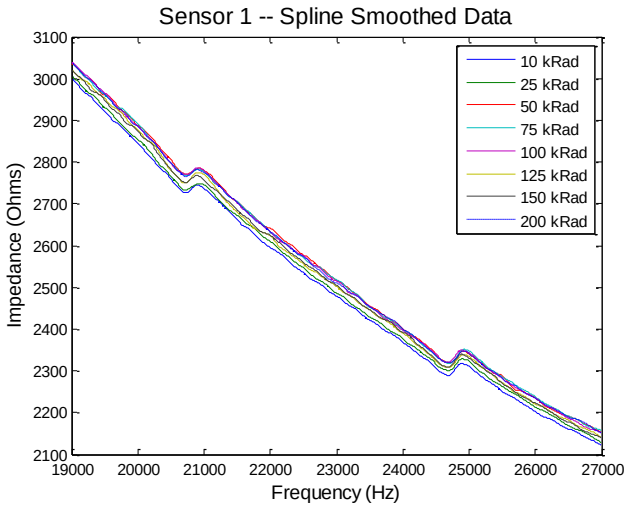

FIGURE 10. SENSOR 1 SPLINE SMOOTHED DATA

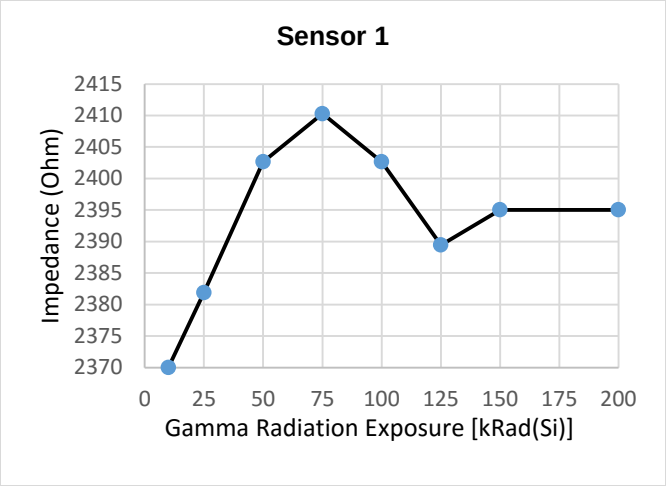

FIGURE 11. SENSOR 1 AMPLITUDE OF IMPEDANCE AT INCREASING GAMMA RADIATION EXPOSURE.

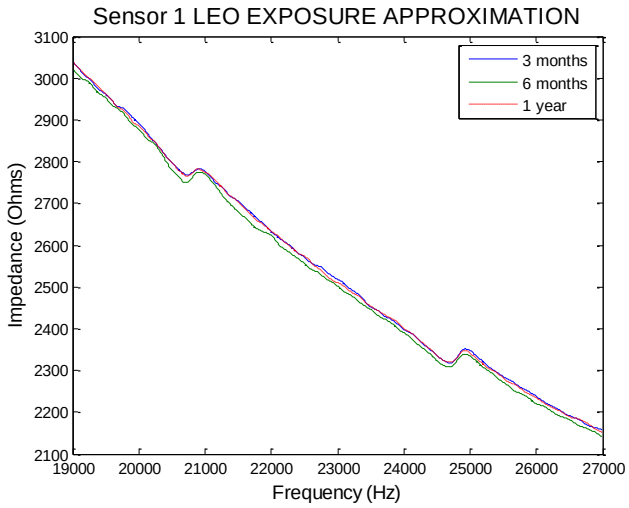

FIGURE 12. SENSOR 1 LOW EARTH ORBIT APPROXIMATION

Sensor 5

Sensor 5 (S5) is the free sensor and reflects only the material properties of the lead-zirconate-titanate (PZT) ceramic. From the graph shown in Figure 13, the resonance of the sensor in moving to higher frequencies. Typically, upward frequency shifts occur at extremely low temperatures [26]. Temperature is not the cause of the frequency shift in this case, as the temperature in the chamber ranged from 14 to 16 degrees Celsius. A two degree temperature shift is not significant enough to cause the frequency change. Figure 14 shows the frequency change as a result of increased gamma radiation absorbed dose. It is proposed that the increased frequency is caused by a reduction of density which is seen in other materials as reported in the introduction. NASA reported in 1970 that some ceramics experienced density loss after exposure to radiation energy over 1 keV [27]. Drawing from NASA's report, the authors used a 1% estimated density loss for the lead-zirconate-titanate ceramic sensor and calculated the change in frequency associated with this density change and arrived at the same ending frequency for Sensor 5 as shown in the graph in Figure 14 (i.e., 238.51 kHz from the starting frequency of 237.31 kHz.)

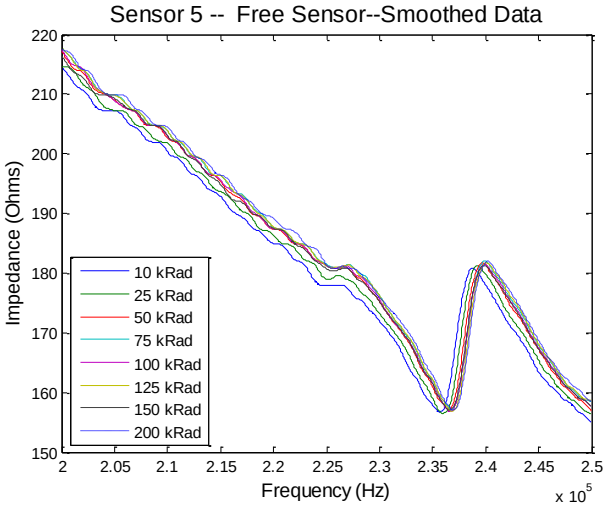

FIGURE 13. SENSOR 5 SPLINE SMOOTHED DATA

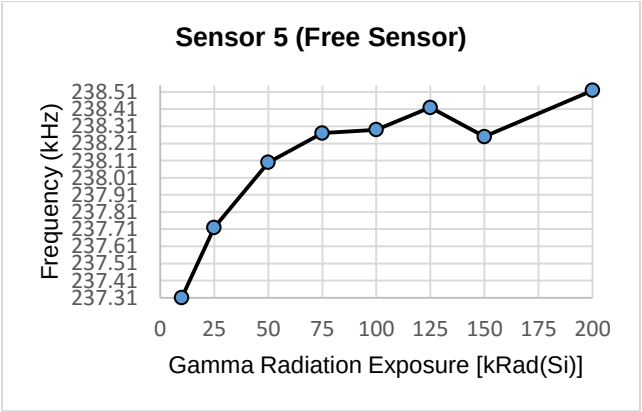

FIGURE 14. SENSOR 5 FREQUENCY AS A RESULT OF INCREASED GAMMA RADIATION EXPOSURE.

ACKNOWLEDGMENTS

Authors would like to acknowledge Federal Aviation Administration (FAA) through Center of Excellence for Commercial Space Transportation for financial support and Dr. Nickolas Demidovich for guidelines in this research. Additional research funding was provided by the New Mexico Space Grant Consortium.

In addition, authors acknowledge the following individuals for their invaluable contribution to reported experimental efforts:

Josh Blundell, Installation Safety Office, Health Physicists, WSMR

Jerame Lopez, Gamma Range Facility Operator, WSMR

Ricardo Ortiz, Gamma Range Facility Specialist/Operator, WSMR

REFERENCES

[1] V. Giurgiutiu and A. and Zagrai, "Damage Detection in Thin Plates and Aerospace Structures with the Electro-Mechanical Impedance Method," *Structural Health Monitoring,* vol. 4, no. 2, pp. 99-118, 2005.

[2] A. Zagrai, D. Doyle, V. Gigineishvili, J. Brown, H. Gardener and B. and Arritt, "Piezoelectric Wafer Active Sensor Structural Health Monitoring of Space Structures," *Journal of Intelligent Materials Systems and Structures,* vol. 21, pp. 921-940, June 2010.

[3] D. Doyle, A. Zagrai, B. Arritt and H. and Cakan, "Damage Detection in Bolted Space Structures," *Journal of Intelligent Material Systems and Structures,* vol. 21, pp. 251-264, February 2010.

[4] G. Musgrave, A. Larsen and T. and Sgobba, Safety Design for Space Systems, Oxford: Elsevier Ltd, 2009.

[5] M. Sajid, N. G. Chechenin, F. S. Torres, E. U. Khan and S. Agha, "Space Radiation Environment Prediction for VLSI Microelectronics Devices Onboard a LEO Satellite Using OMERE-TRAD Software," *Advances in Space Research,* vol. 56, pp. 314-324, 2015.

[6] T. P. O'Brien, J. E. Masur, T. B. Guild and M. D. Looper, "Using Polar-Orbiting Environmental Satellite Data to Specify the Radiation Environment up to 1200 km Altitude," *Space Weather,* vol. 13, pp. 434-445, 2015.

[7] W. E. Price, "The Simulation of Space Radiation Damage to Spacecraft Systems," *IEEE Transactions on Nuclear Science,* vol. 12, no. 6, pp. 2-7, 1965.

[8] European Space Agency, "The Radiation Design Handbook," ESA Publications Division, Noordwijk, 1993.

[9] V. Giurgiutiu and A. Zagrai, "The Use of Smart Materials Technologies in Radiation Environment and Nuclear Industry," in *SPIE 7th International Symposium on Smart Structures and Materials*, Newport Beach, 2000.

[10] H. Lee, H. Sohn, S. Yang and J. Yang, "Monitoring of Pipelines in Nuclear Power Plants by Measuring Laser-Based Mechanical Impedance," *Smart Materials and Structures,* vol. 23, pp. 1-10, April 2014.

[11] S. Delepine-Lesoille, X. Pheron, J. Bertrand, G. Pilorget, G. Hermand, R. Farhoud, Y. Ouerdane, A. Boukenter, S. Girard, L. Lablonde, D. Sporea and V. Lanticq, "Industrial Qualification Process for Optical Fibers Distributed Strain and Temperature Sensing in Nuclear Waste Repositories," *Journal of Sensors,* vol. 2012, pp. 1-9, 2012.

[12] V. Giurgiutiu, X. Buli and L. Weiping, "Development and Testing of High-temperature Piezoelectric Wafer Active Sensors for Extreme Environments," *Structural Health Monitoring,* vol. 9, no. 6, pp. 513-525, 2010.

[13] U. S. Department of Energy, Office of Environmental Management, "Accident Investigation Report, Radiological Release Event at the Waste Isolation Plant on February 14, 2014," Department of Energy, 2014.

[14] A. N. Zagrai and V. Giurgiutiu, Encyclopedia of Structural Health Monitoring, John Wiley & Sons, Ltd., 2009.

[15] D. D. Glower, D. L. Hester and D. F. Warnke, "Effects of Radiation-Induced Damage Centers in Lead Zirconate Titanate Ceramics," *Journal of the American Ceramic Society,* vol. 48, no. 8, pp. 417-421, August 1965.

[16] G. H. Broomfield, "The Effect of Low-Fluence Neutron Irradiation on Silver-Electroded Lead-Zirconate-Titanate Piezoelectric Ceramics," *Journal of Nuclear Materials,* vol. 91, pp. 23-34, 1980.

[17] Y. P. Meleshko, S. G. Karpechko, G. K. Leont'ev, V. I. Nalivaev, A. D. Nikiforov and V. M. Smirnov, "Radiation Resistance of the Piezoelectric Ceramics TsTS-21 and TNV-1," *Atomnaya Energiya,* vol. 61, no. 1, pp. 50-52, July 1986.

[18] B. Lin, M. Gresil, V. Giurgiutiu, T. Knight, A. E. Mendez-Torres and L. Yu, "Nuclear Environmental Effects on Piezoelectric Wafer Active Sensors Based Acousto-Ultrasonic Sensing System," in *Proceedings of ICAPP*, Charlotte, 2014.

[19] E. F. Sturcken, "Irradiation Effects in Magnesium and Aluminum Alloys," *Journal of Nuclear Materials,* vol. 82, pp. 39-53, 1979.

[20] N. Kamigaki, S. Furuno, K. Hojou, K. Ono, E. Hashimoto and K. Izui, "Evolution of Structural Damage in Aluminum Alloys Irradiated with Helium Ions," *Journal of Nuclear Materials,* pp. 191-194, 1992.

[21] D. Hamaguchi and Y. Dai, "Microstructural Change in ALMG3 Alloy Irradiated by Spallation Neutrons and High Energy Protons," *Journal of Nuclear Materials,* pp. 958-962, 2004.

[22] A. Almazouzi, M. Caturla, M. Alurralde, T. Diaz de la Rubia and M. Victoria, "Defect Production and Damage Evolution in Al: A Molecular Dynamics and Monte Carlo Computer Simulation," *Nuclear Instruments and Methods in Physics Research,* pp. 105-115, 1999.

[23] R. L. Sindelar, P. S. Lam, M. R. Louthan and N. C. Iyer, "Corrosion of Metals and Alloys in High Radiation Fields," *Materials Characterization,* vol. 43, pp. 147-157, 1999.

[24] B. Lin, M. Gresil and V. Giurgiutiu, "Structural Health Monitoring with Piezoelectric Wafer Active Sensors Exposed to Irradiation Effects," in *ASME 2012 Pressure Vessels & Piping Division Conference*, Toronto, 2012.

[25] J. W. Howard Jr. and D. M. Hardage, "Space Environments Interactions: Space Radiation and Its Effects on Electronic Systems," National Aeronautics and Space Administration, Marshall Space Flight Center, 1999.

[26] M. L. Anderson, A. N. Zagrai, D. Doyle, D. Hengeveld and M. R. Wilson, "Consideration of Thermal Effects in Electro-Mechanical Impedance Measurements for Space Structures," in *IWSHM 2015*, Stanford, 2015.

[27] National Aeronautics and Space Administration, "Nuclear and Space Radiation Effects on Materials," NASA, 1970.